J Polym Environ (2013) 21:293–302
DOI 10.1007/s10924-012-0516-4

ORIGINAL PAPER

Mechanical, Thermal and Water Absorption Properties of Kenaf-Fiber-Based Polypropylene and Poly(Butylene Succinate) Composites

J. M. Lee · Z. A. Mohd Ishak · R. Mat Taib · T. T. Law · M. Z. Ahmad Thirmizir

Published online: 7 August 2012

Abstract The use of composites made from non-biodegradable conventional plastic materials (e.g., polypropylene, PP) is creating global environmental concern. Biodegradable plastics such as poly(butylene succinate) (PBS) are sought after to reduce plastic waste accumulation. Unfortunately, these types of plastics are very costly; therefore, natural lignocellulosic fibers are incorporated to reduce the cost. Kenaf fibers are also incorporated into PP and PBS for reinforcing purposes and they have low densities, high specific properties and renewable sourcing. However without good compatibilization, the interfacial adhesion between the matrix and the fibers is poor due to differences in polarity between the two materials. Maleic anhydride-grafted compatibilizers may be introduced into the system to improve the matrix-fiber interactions. The overall mechanical, thermal and water absorption properties of PP and PBS composites prepared with 30 vol.% short kenaf fibers (KFs) using a twin-screw extruder were being investigated in this study. The flexural properties for both types of composites were enhanced by the addition of compatibilizer, with improvements of 56 and 16 % in flexural strength for the PP/KF and PBS/KF composites, respectively. Good matrix-fiber adhesion was also observed by scanning electron microscopy. However, the thermal stability of the PBS/KF composites was lower than that of the PP/KF composites. This result was confirmed by both DSC and TGA thermal analysis tests. The water absorption at equilibrium of a PBS composite filled with KFs is inherently lower than of a PP/KF composite because the water molecules more readily penetrate the PP composites through existing voids between the fibers and the matrix. Based on this research, it can be concluded that PBS/KF composites are good candidates for replacing PP/KF composites in applications whereby biodegradability is essential and no extreme thermal and moisture exposures are required.

Keywords Poly(butylene succinate) · Polypropylene · Natural fiber · Compatibilizer · Interface

J. M. Lee · Z. A. Mohd Ishak (✉) · R. Mat Taib · T. T. Law · M. Z. Ahmad Thirmizir
Cluster for Polymer Composites, Engineering and Technology Research Platform, Engineering Campus, Universiti Sains Malaysia, 14300 Nibong Tebal, Pulau Pinang, Malaysia
e-mail: zarifin.ishak@googlemail.com

J. M. Lee · Z. A. Mohd Ishak · R. Mat Taib · T. T. Law · M. Z. Ahmad Thirmizir
School of Materials and Minerals Resources Engineering, Engineering Campus, Universiti Sains Malaysia, 14300 Nibong Tebal, Pulau Pinang, Malaysia

Introduction

At present, conventional plastic materials such as polypropylene (PP) play an essential role in consumers' lives due to their excellent properties. PP exhibits good strength, lightweight, it is easily processed and economical as well. However, the overly wide consumption of plastics in the packaging, agricultural and automobile industries has many implications for the environment. Environmental issues related to the disposal of these non-degradable plastics have attracted increasing concern over the past few decades [1]. Plastics that are not discarded properly not only threaten ecosystems but also pose dangers to human life. Therefore, industrialists and scientists have sought more environmentally friendly alternatives to conventional plastics for their products. Using biodegradable plastics is one of the most viable long term ways to reduce plastic

waste accumulation compared to landfill, recycling and incineration methods.

Polybutylene succinate (PBS) is an aliphatic thermoplastic polyester with many interesting properties including biodegradability, low processing temperature and good mechanical properties [2]. PBS is synthesised by the reaction of the glycol 1,4-butanediol and the aliphatic succinic acid [3]. The degradation of PBS occurs by hydrolysis, whereby the polymer structure is chemically broken down through the metabolism of biological enzymes or microorganisms to form water and carbon monoxide [4, 5]. This material can be degraded in a variety of environments, such as in compost, moist soil and seawater [6]. There are several promising markets for PBS, including packaging films, disposable cups and plates, landfill covers and other low-stress-bearing applications.

Although PBS possesses many attractive properties, it has not yet gained a positive reputation in the market due to its relatively high cost. The incorporation of low-cost natural fibers in PBS composites is able to mitigate this problem by reducing the overall price of the composite material [7]. Natural fibers namely sisal, jute, hemp, flax and kenaf have often been incorporated into various polymer matrices for reinforcement purposes [2, 8]. The primary advantages of using these fibers in plastics are their low densities, low cost, high specific properties and renewable sourcing [9, 10]. In addition, these natural fibers can be naturally degraded by microorganisms.

There have been many reports in the last few decades on the enhancement of composite properties through the incorporation of short natural fibers due to their better processing and easy dispersion [2, 5, 7–11]. However, natural fibers such as kenaf, have very polar hydroxyl groups [2]. This hydrophilic fiber induces higher moisture absorption in the composites and it is detrimental to the compatibility with hydrophobic polymer matrix [1, 9, 12, 13]. Stronger interfacial adhesion between the fiber and the polymer matrix can be promoted through the addition of compatibilizers [9]. As mentioned by Varga et al. [14] and Mohanty et al. [15], compatibilizers can connect the matrix to the fibers with hydrogen or even covalent bonds. For example, the hydrophilic −OH groups in kenaf fibers (KFs) could react with MAPP to form ester linkages. This would in turn, improve the mechanical properties of the composites through better interfacial adhesion.

The aim of this study is to investigate the mechanical, thermal and water absorption properties of PBS composites upon the incorporation of short KFs. The properties of the biodegradable PBS/KF composites were compared to properties of cheaper conventional PP/KF composites. This comparison between the properties of the PP/KF composites and PBS/KF composites is made in order to investigate the possibility of replacing non-degradable PP composites with PBS composites in the aforementioned applications. This paper also examined the role of the compatibilizer in enhancing the mechanical properties. The morphologies of the composites were also examined by SEM to study the interfacial adhesion between the PBS and PP matrices and the KFs.

Experimental

Materials

The PP used was the impact copolymer TITANPRO SM 950, manufactured by Titan Petchem (M) Sdn Bhd (Malaysia). Polybond 3200, a maleated polypropylene (PP-g-MA) obtained from Chemtura Company (Canada) was used as a compatibilizer in this study. The MAH content of the PP-g-MA was 1 wt %, and the polydispersity index calculated from M_n/M_w was 7.9. PBS with the trade name of Bionelle 1020 was obtained from Showa High Polymer (Japan). Kenaf fibers, approximately 2–4 m long, were supplied by the National Kenaf & Tobacco Board (LKTN) (Malaysia). Maleic anhydride (MA) (99 %) and dicumyl peroxide (DCP) (98 %) from Sigma-Aldrich were used for the preparation of the PBS-g-MA compatibilizer. Table 1 summarizes the properties of the raw materials specified by the manufacturers' material datasheets.

Kenaf Fiber Preparation

Long bundles of KFs were cut into shorter sections approximately 1 cm in length using metal paper cutters. These fibers were then fed into a grinder with a fixed 3 mm diameter sieve. The moisture was removed by drying the fiber in a vacuum oven at 80 °C for 24 h before compounding. The length distribution of 200 randomly selected fibers collected before and after the compounding process was measured using an image analyzer model SXGA with stereo-zoom and analysis software VIP Plus. The fiber length distribution before and after compounding is shown by a frequency distribution graph. The fibers from PP/KF and PBS/KF composites were extracted using the dissolution method where the xylene solution was used to dissolve

Table 1 Material properties of raw materials

Materials	MFI (g 10 min^{-1}) (2.16 kg, 190 °C)	Density (g cm^{-3})
PP	21	0.90
PBS	25	1.25
PP-g-MA	115	0.91

Data from manufacturer

the PP matrix while the chloroform solution was used to dissolve PBS matrix. The critical length of the fibers, l_c, to strengthen a material to its maximum potential is estimated by Eq. 1,

$$l_c = \left(\frac{\sigma_f d}{\tau_c}\right) \quad (1)$$

where σ_f is the tensile strength of the fiber, d is the diameter of the fiber, and τ_c is the shear strength of the bond between the matrix and the fiber.

PBS-g-MA Preparation

The grafting reaction was conducted in a Haake Polydrive Mixer Rheomix R600/610 with two counter rotating roller blades at a temperature of 130 °C and a rotor speed of 50 rpm. PBS, MA and DCP were premixed at a ratio of 100:5:1 phr before being fed into the mixer. The grafted polymer was refluxed in chloroform for 1 h before being filtered into cold methanol to form a white precipitate. The precipitate was then washed repeatedly with fresh methanol to remove any unreacted MA. The polymer was collected and dried in a vacuum oven at 80 °C for 24 h [16].

FTIR Spectrometry

Solid PBS-g-MA was used as a compatibilizer in this study. An FTIR spectrometer (Perkin Elmer System 2000) was used to analyze the MA powder and the purified PBS-g-MA. The powder was mixed with KBr before being compressed under a constant pressure of 3.45×10^6 Nm^{-2} for 1 min to form thin pellets. The spectra were obtained in transmission mode at a resolution of 4 cm^{-1} with 32 scans per sample in the mid-IR range of 600–4,000 cm^{-1}.

Composite Production

Table 2 shows the formulations for each compound. Predetermined processing parameters were selected for the compounding process. A twin screw counter-rotating extruder machine (Model PSW30) was used for mixing the matrix with the natural fiber. The mixing temperature for the PP composites was fixed from zone 1 to zone 10 at 155–175 °C and the screw speed was maintained at 100 rpm. As for PBS, the temperature was fixed at 110–130 °C and the screw speed was maintained at 50 rpm. The side feeder was used for feeding the KFs into the melt blend within the extruder.

Mechanical Testing

The samples for testing flexural strength were prepared using a hot compression molding machine (Kao Tieh Gotech). A mold with specific dimensions of $120 \times 12 \times 3$ mm^3 (length × width × thickness) was used for the sample preparation. For PP composites, the molding cycle involved 5 min for preheating, 3 min for compression under pressure 6.89×10^6 Nm^{-2} and 5 min for cooling. For PBS composites, the molding cycle involved 10 min for preheating, 4 min for compression under pressure and 4 min for cooling. The temperatures for upper and lower mold were 185 and 130 °C for PP and PBS composites, respectively. Prior to testing, the specimens were conditioned at room temperature in a desiccator for 24 h.

Flexural tests were performed in three-point bending mode using a Universal Testing Machine (UTM, Instron-3366) at a crosshead speed of 5 mm/min and span length of 50 mm. The static bending tests were performed according to ASTM D 790-10. For every set of formulations, 5 specimens were tested to determine the average properties. The tests were conducted at a standard laboratory atmosphere of 23 °C (±2 °C).

Thermal Analysis

The crystallization and melting behaviors of the composites were determined using a Perkin Elmer DSC-7. An initial scan was conducted on samples weighing 10-15 mg at a temperature range of 30–200 °C with a heating rate of 10 °C/min under a flow of nitrogen gas. The temperature scan was then continued with cooling to 30 °C and subsequent heating to 200 °C in the second scan. The melting point, T_m, and heat of fusion, ΔH_m, were evaluated from the maximum point of the endothermic peak and the area under the DSC curves from the second scan. The degree of crystallinity, χ_c was calculated from Eq. 2:

Table 2 Formulations for the PP/KF and PBS/KF composites

Denotations	Matrix (vol.%)	KF (vol.%)	PP-g-MA (vol.%)	PBS-g-MA (vol.%)
PP	100	–	–	–
PP/KF	70	30	–	–
PP/KF/MA	65	30	5	
PBS	100	–	–	–
PBS/KF	70	30	–	–
PBS/KF/MA	65	30	–	5

The vol.% of KF reported was the amount of dry fiber in the compound

For pure PP or PBS,

$$\chi_c(\%) = \frac{\Delta H_f}{\Delta H_f^0} \times 100\,\%$$

and for KF-filled composites,

$$\chi_c(\%) = \frac{\Delta H_f}{\Delta H_f^0(1 - W_f)} \times 100\,\% \quad (2)$$

where ΔH_f is the heat of fusion for PP, PBS and the composites. ΔH_f^0 is the heat of fusion for 100 % crystalline PBS (ΔH_{100} = 110.3 J/g) [17] or for 100 % crystalline PP (ΔH_{100} = 207.1 J/g) [18]. W_f is the weight fraction by unity of the KFs in the composite.

The thermal decomposition stabilities of PBS composites were analyzed using thermogravimetric analysis Perkin Elmer TGA on samples weighing 10–15 mg. The heating rate was 10 °C/min over a temperature range from 30 to 600 °C, under purging nitrogen of 20 ml/min.

Water Absorption Test

The water absorption behavior was tested according to ASTM D 570. The flexural test specimens were dried in a vacuum oven until a constant weight was attained prior to the test. All specimens were immersed in distilled water at ambient temperature for 60 days. At predetermined intervals, specimens were removed from the water and the surfaces were blotted with a clean cloth before the sample weights were measured. The average values of results from 6 specimens were attained. The water uptake at a given time interval was determined using Eq. 3:

$$M_t(\%) = \frac{W_w - W_d}{W_d} \times 100 \quad (3)$$

where, M_t, is the water absorption at a given time, t, and W_d and W_w are the weight of specimen before and after immersion respectively.

The diffusion coefficient, D, can be calculated from the initial slope of the plot of water uptake against time using Eq. 4:

$$D = \frac{\pi h^2 (M_2 - M_1)^2}{16 M_m^2 (t_2^{1/2} - t_1^{1/2})^2} \quad (4)$$

where M_1, and M_2 are the water content at time t_1 and t_2 respectively. M_m is the maximum water content, also known as equilibrium water content, and h is the thickness of the sample.

Scanning Electron Microscopy

A morphological study of the fractured surface was performed by taking scanning electron micrographs at predetermined magnifications using a field emission scanning electron microscope (FESEM, model VPFESEM Supra 35VP). Prior to SEM observations the specimens were sputter coated with gold–palladium sputter coater Polaron Sc515 to prevent electrical charging. The morphological study was used to observe the matrix-fiber interfacial adhesion.

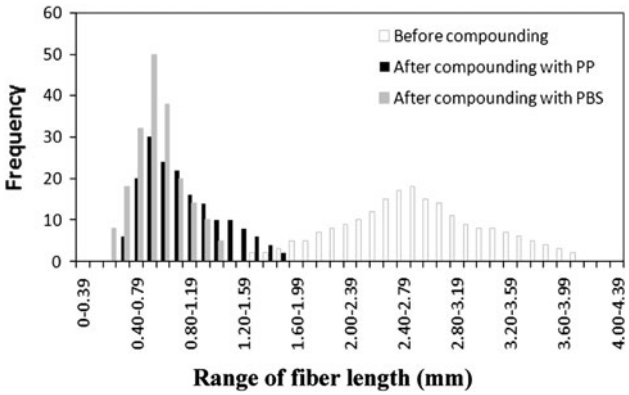

Fig. 1 Fiber length distribution before and after compounding

Results and Discussion

Fiber Length Distribution

Processing equipment such as the twin screw extruder imposes stresses and high shearing upon the fibers that is sufficient to cause mixing, fiber breakage and bundle separation [19]. Most of fiber breakage occurs in the transition element of a twin screw extruder. Screw designs that have greater residence times and mixing capabilities induce more fiber breakage [20]. The extent of fiber breakage during compounding is crucial, as the fiber length determines the reinforcing capabilities of the fiber. The distribution plots of the KF lengths before and after compounding are shown in Fig. 1. Prior to processing, 94 % of the short KFs fell mostly within the range of 1.5–3.5 mm. However for both the PP and PBS composites, the majority of these fibers broke into shorter lengths ranging from 0.4 to 0.8 mm after subjected to mixing process. A narrower fiber length distribution after processing was also observed.

Characterisation of PBS-g-MA (FTIR)

The in situ melt grafting of MA onto the PBS matrix was performed in a Haake Rheomixer. The graft content of the compatibilizer is affected by many factors including the concentration of maleic anhydride and dicumyl peroxide, the temperature and the residence time [9]. Selecting the optimum conditions for the grafting process is crucial in

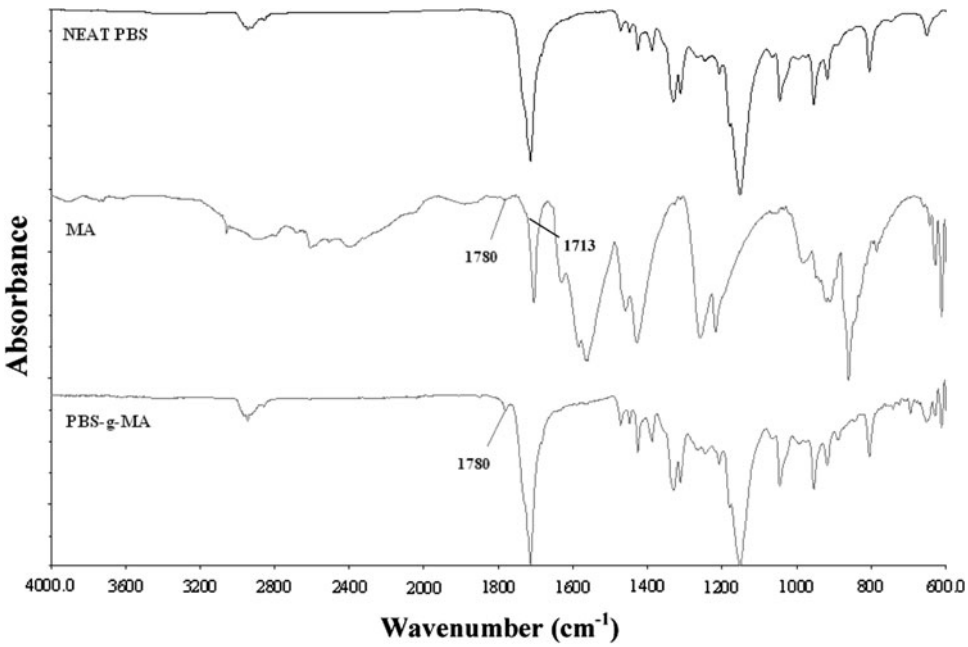

Fig. 2 FTIR spectra of MA and grafted PBS-g-MA after purification

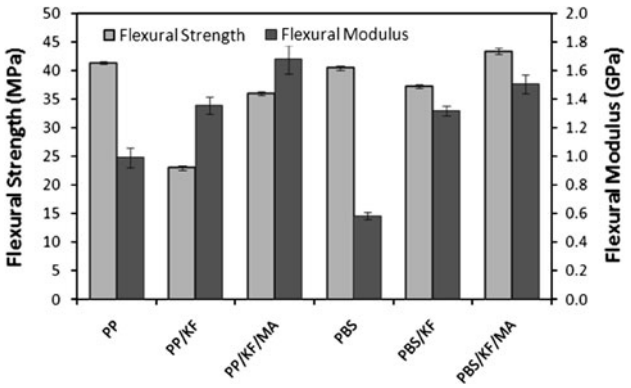

Fig. 3 Flexural strengths and moduli of the PP/KF and PBS/KF composites

synthesising a compatibilizer with sufficient graft content. As proposed by Carlson et al. [21], only a small amount (3–5 wt %) of anhydride grafted onto the polymer chain is required to improve the interfacial adhesion of the composite components. This result is confirmed in this study as the addition of 5 % PBS-g-MA in the composite was found to improve the fiber-matrix interfacial adhesion substantially. [7].

After purification, the PBS-g-MA was analyzed by FTIR. The IR spectrum is presented in Fig. 2. The absorptions at 1,713 and 1,780 cm^{-1} are the characteristic bands of the acid carbonyls and anhydride carbonyls respectively [21]. The band for the succinic anhydride group band observed at 1,780 cm^{-1} of PBS-g-MA spectrum confirms the reaction in the grafting process. The graft content determined from the acid titration method as suggested by Thirmizir et al. [5] was found to be 1.20 + 0.05 %.

Flexural Properties

The flexural properties of the PP/KF and PBS/KF composites are represented in Fig. 3. The flexural strength of neat PP is 41.35 MPa. A 43 % reduction in flexural strength was apparent for the PP composite upon the addition of 30 vol.% KF. This downward trend in flexural strength was also observed for the PBS/KF composites. With the addition of the KFs into the PBS matrix, the flexural strength deteriorated from 40.5 to 37.3 MPa, a loss of 7.9 %. The strength of the kenaf-filled composites decreased due to the weak interfacial bonding between the hydrophilic kenaf fibers and the hydrophobic PP or PBS matrices. Weak matrix-fiber interfaces act as stress concentration sites for fracture in the composites during mechanical testing [22, 23, 25]. The decrease in strength may also be attributed to detrimental microcrack initiation upon the incorporation of the kenaf fibers [10]. In addition, severe fiber attrition during compounding reduced the reinforcing capability of the fibers, as mentioned previously in "Fiber length distribution" section. The composite properties are a function of fiber length because the stress imposed on the short fiber ends cannot be neglected. Fiber breakage should not shift the distribution below the critical fiber length, as this will reduce the reinforcing capability of the fiber [1]. When the fiber lengths are below the critical fiber length, the stress transfer from the matrix to the fiber is insufficient to enhance the material fracture strength.

If the interfacial shear strength is equal to matrix shear strength as estimated from the von-Mises yield criterion, using polymer tensile strength of 17.5 MPa (for PP) and 34.0 MPa (for PBS) obtained from our previous findings, the shear strength of the bond between the matrix and the fiber is measured to be 10.1 and 19.6 MPa respectively. With the assumption that the kenaf fiber strength is about 215 MPa as reported by Edeerozey et al. [24] and that the "diameter" of the fiber bundle is 70 μm as obtained from a study by Thirmizir et al. [5], the critical fiber length is approximately 1.490 mm for the PP composites and 0.768 mm for the PBS composites.

The majority of the fiber lengths after compounding were found to be in the range of 0.5–0.7 mm as presented in Fig. 1. Approximately 68 % of the fiber lengths in the PBS composites fall were above the critical fiber length, while for the PP composites, merely 10 % of the fiber lengths fall were above the critical fiber length. This indicates that the short fibers in the PP composite are unable to transfer stress effectively, in agreement with the significant reduction in flexural strength obtained for the PP/KF composite. To strengthen the PP composites through the incorporation of KFs, longer fiber lengths must be maintained.

Additionally, the critical value l_c is inversely proportional to the interfacial strength between the matrix and the fibers [1]. Poor interfacial bonding between the matrix and the fibers may result in voids or stress concentrators in the composite within a continuous phase. These 'gaps' affect the mechanical properties of the composites as demonstrated by Baiardo et al. [1]. Hence, good interfacial bonding between the fiber and the matrix is especially important for composites with shorter fibers. The better interfacial adhesion observed in composites with compatibilizers will reduce the minimum critical fiber length required for effective stress transfer in high loading applications.

The interactions between the matrix and the natural fiber, could be promoted with the addition of MA-g-compatibilizers as demonstrated by the increase in flexural strength. This result is similar to the findings of Kim et al. [26]. The flexural strength of the PBS-g-MA compatibilized PBS/KF composite was found to be the highest. The addition of PBS-g-MA into the composite system has induced an increase of 16.5 % in flexural strength compared to the composite without compatibilizer.

The flexural modulus of PP composites increased by 126 % from 0.6 to 1.3 GPa upon the addition of the KF. The compatibilized PP/KF composite exhibited the highest flexural modulus of 1.7 GPa. The flexural modulus of the PBS/KF composite with the Compatibilizer exhibited some improvement as well, reaching 1.5 GPa. When natural fibers such as kenaf were incorporated into composites, the segmental movement of the polymer chains was hindered. Hence, the composites become stiffer, increasing their flexural moduli. The increase in flexural moduli is also attributed to the existing chemical constituents in KFs such as lignin, which binds the kenaf fibers together, and cellulose, which stiffens the kenaf fiber cell wall [27]. Although PBS/KF composites possessed lower flexural modulus than PP/KF composites, the flexural strength of PBS/KF composite was reportedly higher. This was because the fiber length is also a critical factor in reinforcing a composite. Although the KF was able to contribute to the stiffness of the composite, the better reinforcing effects could be achieved if the average fiber length exceeds the critical fiber length.

The flexural strength and modulus increase upon the addition of the compatibilizer because of the high degree of interactions between the KFs and the matrices. The polymer matrix adhered well to the KFs, hindering the movement of the polymeric chains in the composites. According to Varga et al. [14], compatibilizers can connect the matrix to the fibers with hydrogen or even covalent bonds. This would improve the mechanical properties of the components through improved interfacial adhesion as the load can be transferred from the matrix to KFs more efficiently. Additionally, the overall increase in the modulus of filled composite is in agreement with reports by Ratto et al. [28]. Better wetting of the KFs by the matrix in the compatibilized system was observed in the SEM micrographs (see Figs. 7b, 8b), which exhibited better matrix-fiber contact and fewer interfacial voids.

Crystallization and Melting Behavior

Thermal results including melting temperature (T_m) and crystallization temperature (T_c) obtained through DSC are displayed in Table 3. PP and PBS are semicrystalline polymers that consist of amorphous and crystalline regions in the structure. The T_c temperature observed for the PP was higher than that for the PBS. These matrices had crystallization temperature of 118.2 and 77.0 °C, respectively. The T_c shifted to higher temperature after the

Table 3 Effects of KFs and compatibilizers on the crystallization and melting behavior of the PP and PBS composites

Sample	T_c (°C)	T_m (°C)	χ_c (%)
PP	118.2	163.8	39.9
PP/KF	119.2	162.2	34.7
PP/KF/MA	119.2	161.4	34.2
PBS	77.0	115.3	58.1
PBS/KF	81.4	114.5	51.8
PBS/KF/MA	81.6	114.1	70.6

addition of the KFs. This shift in T_c was related to crystallization rate and extent of crystallinity as mentioned by Kim et al. [6]. These T_c temperatures were unchanged upon the addition of MA-grafted compatibilizers to the composite. The melting temperatures of the PP and PBS composites were not significantly altered through the addition of KFs and compatibilizers. Similar trend were reported by Kim et al. [26] for bio-flour filled PP composites. The T_m values of the PP composites were also higher compared to those of the PBS composites.

The crystallinity of the PP composites, χ_c decreased upon the addition of KFs because the natural fibers restrict the molecular motion of the matrix, preventing the formation of PP crystallites and confining the polymer chain orientation [10, 13]. On the contrary, the structure of PBS-g-MA increased the crystallinity of the composite [29]. This suggested that the composites compatibilized with PBS-g-MA have higher crystallization behavior than non-compatibilized composites. According to Kim et al. [26], the higher crystallinity of composites with MA was contributed from the better dispersion of the compatibilizer in the matrix as well as higher chain branching of MA.

Thermal Degradation

The weight loss versus temperature curves of the PP/KF and PBS/KF composites obtained from TGA are illustrated in Fig. 4. Three distinct regions can be observed in these curves. The initial weight loss occurred between 50 and 100 °C. This small drop in weight resulted from the loss of moisture from the KFs. In the second stage from 200 to 400 °C, the main degradation of all three components, PP, PBS and KF was observed. KF was degraded within the range of 244–372 °C, followed by neat PBS within the range of 343–443 °C and neat PP within the range of 374–483 °C, accordingly. The final region consists of residual carbon species from the degraded KFs. [30].

The thermal stability degradation curves of the PP/KF composites falls between that of the PP matrix and the KFs.

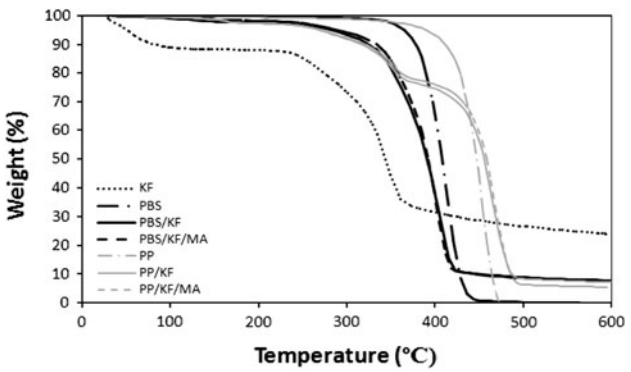

Fig. 4 TGA thermograms of the PBS/KF composites

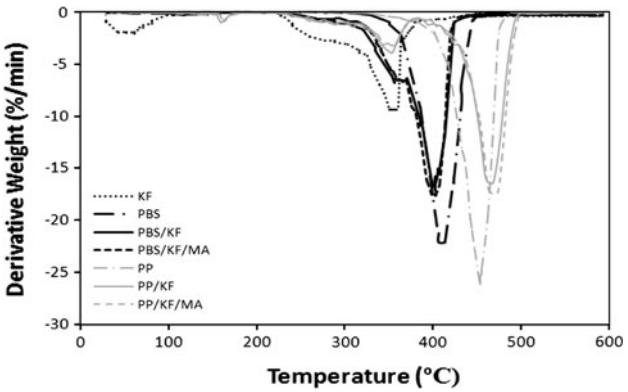

Fig. 5 DTG thermograms of the PBS/KF composites

Similar finding were discovered for the PBS/KF composites. The thermal stability of the composites is reduced due to the incorporation of the KFs. The lower onset degradation temperature of KF contributed to the lower thermal stability in KF incorporated composites. An analogous trend was reported by Lee et al. [12] in their research on PBS composites with natural bamboo fiber.

From the derivative weight plot in Fig. 5, two main peak temperatures are observed. The PP matrix degrades at a peak temperature of weight loss at 454 °C while for PBS matrix, the peak temperature of weight loss was at 414 °C. This is due to the low thermal stability of PBS matrix as compared to PP matrix. The KF had the lowest peak temperature at 355 °C. Therefore, the introduction of KFs inherently reduces the thermal stability of the composites. For the KF-filled composites, the first shoulder peak in the temperature range of 350–370 °C indicates the degradation of cellulose, hemicelluloses and lignin from the KFs and the second prominent peak corresponds to the depolymerisation of the PP or PBS matrix (refer Table 4) [31]. Table 4 summarizes the peak temperatures of the composite specimens, including the neat PBS and KFs in the DTG curves from Fig. 5. For PBS composites filled with KF composites, the primary peak representing the degradation of KF was reported to be higher than the actual

Table 4 Peak temperatures from derivative weight curves for the PP/KF and PBS/KF composites

Sample	Primary peak temperature (°C)	Secondary peak temperature (°C)
KF	56.25	355.74
PP	453.74	–
PP/KF	350.99	465.73
PP/KF/MA	351.27	469.12
PBS	413.88	–
PBS/KF	370.84	403.08
PBS/KF/MA	367.71	404.48

degradation temperature for KF whereas the secondary peak representing the degradation of PBS was reported to be lower than the degradation temperature for neat PBS. This is because the less thermally stable KF can be compensated by the PBS matrix while the higher thermal stability of the PBS matrix was compromised by the existence of KF [9]. The primary peak temperature for PBS/KF composites was higher than PP/KF composites although the pure matrices showed the opposite trend.

It is interesting to note that the compatibilized PBS composite has lower peak temperature than uncompatibilized composite. This trend was not observed in PP composite. Araujo et al. [32] mentioned that the greater interaction between fiber and matrix could promote the degradation process of the two components. The reason to that was the rapid degradation of one component would accelerate the thermal degradation of neighboring component. Another valid reason for the less stable MA compatibilized PBS composite was the presence of peroxide residue used for grafting process. This is possible as the MA-g-PBS was self-synthesised.

Water Absorption Behavior

Although KFs are relatively cheap and are promising materials for incorporation in biodegradable composites such as PBS, its hydrophilic nature may render the composites high in moisture absorption. In this study, the moisture absorption behavior of PBS and PP filled with KFs was investigated. The percentage of water absorbed was plotted against the square root of time as represented in Fig. 6. The moisture uptake increased with the square root of time for PP and PBS composites. Water absorption for all the composites occurred predominantly within the first 100 h. Once the samples reached water saturation, the absorption rates slowed down and finally reached equilibrium. This demonstrates that the pattern of the water absorption curve followed Fick's second law [33].

The values of D and M_m (Eqs. 3, 4) for the PP/KF and PBS/KF composites are tabulated in Table 5. The equilibrium moisture uptake, M_m for neat PP and PBS were very low due to the hydrophobic nature of the materials. The addition of KFs to the PP and PBS matrices increased the values of D and M_m dramatically. Higher water diffusion was observed in the composite due to the tendency of the KFs to absorb water. The accessible hydroxyl groups in the cellulose fiber have been reported to promote hydrogen bonding with water molecules, thus, increasing the moisture content [34, 35]. The reduced intermolecular bonding between the fiber and the matrix could lead to deterioration of the mechanical properties for the wet composites [9, 12, 36] Some literature reports have indicated that better interaction of natural fiber and polymer matrix with the

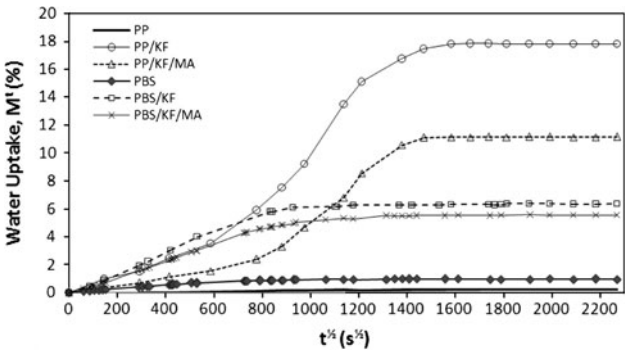

Fig. 6 Water absorption curves of the PP/KF and PBS/KF composites over 60 days of water immersion

presence of a compatibilizer could reduce the existing gaps between the fiber and the matrix, thus restricting the pathway for water within the composite [37]. This finding was also observed in the compatibilized PP/KF composites. Compatibilizers create better interaction between the matrix and the fiber. Hence, fiber wetting by the PP matrix was more effective. The better encapsulation of the fiber by matrix inherently reduces the water absorption of the composite by suppressing the number of accessible hydroxyl groups when the composite is exposed to water [38]. Furthermore, the formation of ester linkages between the MA functional groups and the hydroxyl groups of the KFs could contribute to the lower water uptake by the composite, as mentioned by Mohanty et al. [15]. The PBS/KF composites had lower water absorption at equilibrium compared to the PP/KF composites. This is probably due to the larger separation between the fiber and PP matrix which could act as capillaries for water to travel across the bulk of the PP/KF composites. High water absorption in composites causes undesirable losses in material mechanical properties. The mechanical properties after water absorption will be the subject of our forthcoming publications based on the hydrolytic degradation of these composites at various temperatures. These detrimental effects are derived from debonding, delamination and cracking in composites subjected to prolonged immersion in water [39].

Morphological Analysis

The SEM micrographs in Figs. 7, 8 reveal KFs protruding from the fractured surfaces of the PP and PBS composites. Poor interfacial adhesion was clearly observed in the small gaps between the matrix and the fibers for the PP/KF composites without the addition of PP-g-MA (see Fig. 7a). Similar debonding of the fibers from the matrix was also observed in the PBS/KF composites as indicated in Fig. 8a. As discussed previously, the PP and PBS matrices have low compatibility with KF due to differences in polarity. Therefore, these matrices were unable to provide good

Table 5 Time taken to achieve equilibrium, water absorption at equilibrium (M_m) and diffusion coefficient (D) obtained from water absorption testing of the PP/KF and PBS/KF composites

Sample	Time taken to achieve equilibrium, t_m (h)	Water absorption at equilibrium, M_m (%)	Diffusion coefficient, D ($\times 10^{-12}$ m^2/s)	Slope of log (M_t/M_m) vs. log t, n
PP	147	0.10 ± 0.01	0.10 ± 0.01	0.380
PP/KF	803	17.82 ± 0.45	1.26 ± 0.15	0.713
PP/KF/MA	625	11.13 ± 0.53	0.87 ± 0.12	0.582
PBS	250	0.97 ± 0.03	1.45 ± 0.21	0.486
PBS/KF	369	6.37 ± 0.29	2.47 ± 0.20	0.729
PBS/KF/MA	323	5.56 ± 0.24	2.07 ± 0.20	0.568

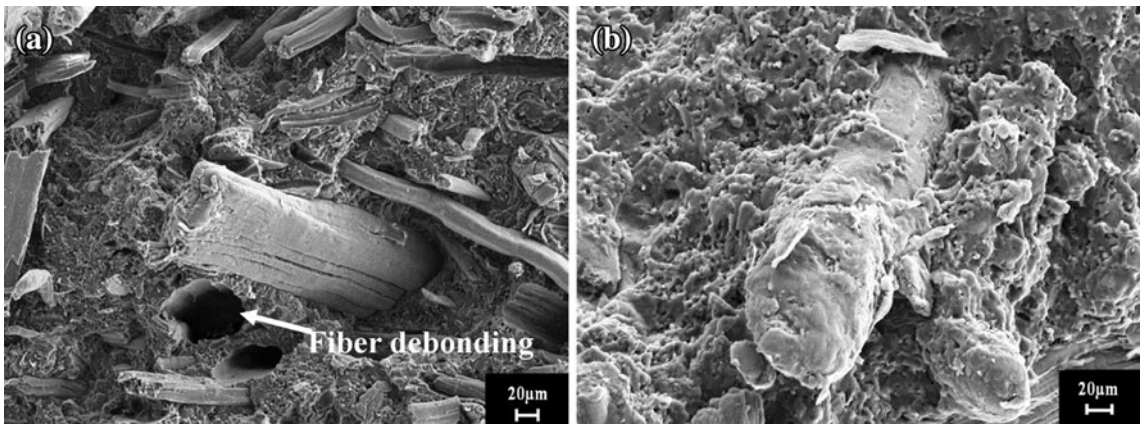

Fig. 7 SEM micrographs of the flexural fracture surface of the PP/KF composites **a** without PP-g-MA, and **b** with PP-g-MA

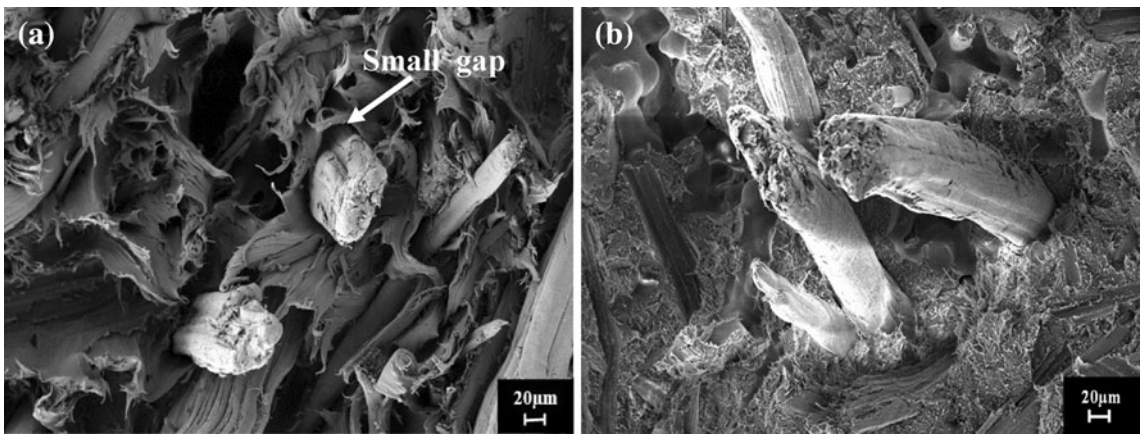

Fig. 8 SEM micrographs of the flexural fracture surface of the PBS/KF composites **a** without PBS-g-MA and **b** with PBS-g-MA

wetting for the fibers without the introduction of a compatibilizer.

Compatibilizers were introduced to promote better adhesion between the fibers and the polymer matrix. As a result, the fiber-matrix gap was nearly absent, clearly showing that PP-g-MA and PBS-g-MA do induce better wetting of the KFs with the matrix, as shown in Figs. 7b, 8b respectively. As reported by Bledzki et al. [38], fiber pull out and debonding during fracture were reduced tremendously due to the compatibilization effect. Stronger interaction may effectively transfer and disperse stress, thus improving the mechanical properties of the composites, as seen in Fig. 3 [2, 22].

Conclusions

The flexural strengths of PP and PBS composites deteriorated with the addition of KFs to the systems. However, the flexural strength improved significantly with the aid of MA-grafted

compatibilizers. This is mainly due to improved interfacial bonding between the matrix and the fibers. The flexural moduli were also found to increase in KF-filled composites. However, there were several disadvantages to incorporating natural fibers such as kenaf in a composite. The thermal stability was reduced and the water absorption rate was greater for the composites with addition of KFs. With compatibilization, the thermal stability of a composite was maintained, but the water uptake was reduced, even with prolonged immersion in water. PBS composites possessed higher flexural strength and lower water absorption at equilibrium as compared to PP composites. However, the PBS composites had lower thermal degradation temperature as proven from the TGA analysis. These results display the potential utility for PBS composites in replacing PP composites in applications that do not require extreme thermal exposure and where biodegradability is of crucial consideration.

Acknowledgments The authors would like to express their appreciation to Forest Research Institute Malaysia (FRIM) for supplying machines for processing kenaf fibers for this course of study. They would also like to extend their gratitude to USM FELLOWSHIP (1001/441/CIPS/JHEA/AUPE001), Research Universiti Postgraduate Research Grant Scheme USM-RU-PRGS (1001/PBAHAN/8034002) and RU Cluster Grant (1001/PKT/8640012) for funding this research.

References

1. Baiardo M, Zini E, Scandola M (2004) Compos Part A 35:703–710
2. Liu L, Yu J, Cheng L, Yang X (2009) Polym Degrad Stabil 94:90–94
3. Kim HS, Yang HS, Kim HJ (2005) J Appl Polym Sci 97:1513–1521
4. Wang H, Ji J, Zhang W, Zhang Y, Jiang J, Wu Z, Pu S, Chu PK (2009) Acta Biomater 5:279–287
5. Ahmad Thirmizir M, Mohd Ishak ZA, Mat Taib R, Rahim S, Jani S (2011) J Appl Polym Sci 122:3055–3063
6. Kim HS, Kim HJ, Lee JW, Choi IG (2006) Polym Degrad Stabil 91:1117–1127
7. Ahmad Thirmizir MZ, Mohd Ishak ZA, Mat Taib R, Rahim S, Mohamad Jani S (2011) J Polym Environ 19:263–273
8. Shinji O (2008) Mech Mater 40:446–452
9. Tserki V, Matzinos P, Panayiotou C (2006) Compos Part A 37:1231–1238
10. Lee SM, Cho D, Park WH, Lee SG, Han SO, Drzal LT (2005) Compos Sci Technol 65:647–657
11. Xue Y, Du Y, Elder S, Wang K, Zhang J (2009) Compos Part B 40:189–196
12. Lee SH, Wang S (2006) Compos Part A 37:80–91
13. Wu CS (2009) Polym Degrad Stabil 94:1076–1084
14. Varga CS, Miskolczi N, Bartha L, Lipoczi G (2010) Mater Des 31:185–193
15. Mohanty AK, Misra M, Drzal LT, Selke SE, Harte BR, Hinrichsen G (2005) Natural fibers, biopolymers, and biocomposites. CRC Press, p 875
16. Mani R, Bhattacharya M, Tang J (1999) J Polym Sci 37:1693–1702
17. Phua YJ, Chow WS, Mohd Ishak ZA (2011) Polym Degrad Stabil 96:1194–1203
18. Shi Y, Chen F, Yang J, Zhong M (2010) Appl Clay Sci 50:87–91
19. Beg MDH, Pickering KL (2008) Compos Part A 39:1091–1100
20. Keller A (2003) Compos Sci Technol 63:1307–1316
21. Carlson D, Nie L, Narayan R, Dubios P (1999) J Appl Polym Sci 72:477–485
22. Sharifah HA, Martin PA (2004) Compos Sci Technol 64:1219
23. Sharifah HA, Martin PA (2004) Compos Sci Technol 64:1231
24. Edeerozey AM, Hazizan MA, Azhar AB, Zainal Ariffin MI (2007) Mater Lett 61:2023
25. Oksman K, Skrifvars M, Selin JF (2003) Compos Sci Technol 63:1317–1324
26. Kim HS, Lee BH, Choi SW, Kim S, Kim HJ (2007) Compos Part A 38:1473–1482
27. Adhikary KB, Pang S, Staiger MP (2008) Compos Part B 39:807–815
28. Ratto JA, Stenhouse PJ, Auerbach M, Mitchell J, Farrell R (1999) Polymer 40:6777–6788
29. Ray SS, Bandyopadhyay J, Bousmina M (2007) Polym Degrad Stabil 92:802–812
30. Ndazi BS, Karlsson S (2011) eXPRESS Polym Lett 5:119–131
31. Lee BH, Kim HS, Lee S, Kim HJ, Dorgan JR (2009) Compos Sci Technol 69:2573–2579
32. Araujo JR, Waldman WR, De Paoli MA (2008) Polym Degrad Stabil 93:1770–1775
33. Wan YZ, Luo H, He F, Liang H, Huang Y, Li XL (2009) Compos Sci Technol 69:1212–1217
34. Ahmad Thirmizir M, Mohd Ishak ZA, Mat Taib R, Sudin R, Leong YW (2011) Polym-Plast Technol 50:339–348
35. Athijayamani A, Thiruchitrambalam M, Natarajan U, Pazhanivel B (2009) Mater Sci Eng 517:344–353
36. de Albuquerque AC, Joseph K, Hecker de Carvalho L, d'Almeida JRM (2000) Compos Sci Technol 60:833–844
37. Kazemi NS, Kiaefar A, Hamidina E, Tajvidi M (2007) J Reinf Plast Comp 26:341
38. Bledzki AK, Mamun AA, Faruk O (2007) eXPRESS Polym Lett 1:755–762
39. Tajvidi M, Najafi SK, Moteei N (2006) J Appl Polym Sci 99:2199–2203